

## Integrated modeling of steady-state scenarios for ITER: physics and computational challenges

G. Giruzzi<sup>1</sup>, J.M. Park<sup>2</sup>, M. Murakami<sup>2</sup>, C.E. Kessel<sup>3</sup>, A. Polevoi<sup>4</sup>, A.C.C. Sips<sup>5</sup>, J.F. Artaud<sup>1</sup>, V. Basiuk<sup>1</sup>, P. Bonoli<sup>6</sup>, R.V. Budny<sup>3</sup>, A. Fukuyama<sup>7</sup>, J. Garcia<sup>1</sup>, N. Hayashi<sup>8</sup>, M. Honda<sup>8</sup>, S. Ide<sup>8</sup>, F. Imbeaux<sup>1</sup>, E. Joffrin<sup>9</sup>, T. Luce<sup>10</sup>, Y-S. Na<sup>11</sup>, T. Oikawa<sup>4</sup>, T. Ozeki<sup>8</sup>, R. Prater<sup>10</sup>, M. Schneider<sup>1</sup>, H. St.John<sup>10</sup>, A.A. Tuccillo<sup>12</sup>, ITPA/Steady-State Operation Group

<sup>1</sup> CEA, IRFM, F-13108 Saint-Paul-lez-Durance, France

<sup>2</sup> Oak Ridge National Laboratory, Oak Ridge, Tennessee, USA

<sup>3</sup> Princeton Plasma Physics Laboratory, Princeton, NJ, USA

<sup>4</sup> ITER Organization, Building 519, Cadarache, 13108 St. Paul-lez-Durance, France

<sup>5</sup> Max-Planck-Institut für Plasmaphysik, EURATOM-Assoziation, Garching, Germany

<sup>6</sup> Plasma Science and Fusion Center, MIT, Cambridge, USA

<sup>7</sup> Dept. of Nuclear Engineering, Kyoto University, Kyoto, Japan

<sup>8</sup> Japan Atomic Energy Agency, Naka, Ibaraki, Japan

<sup>9</sup> JET-EFDA Culham Science Centre, Abingdon, UK

<sup>10</sup> General Atomics, San Diego, CA, USA

<sup>11</sup> Dept. of Nuclear Engineering, Seoul National University, Seoul, 151-744 Korea

<sup>12</sup> Associazione EURATOM-ENEA, CR ENEA-Frascati, Rome, Italy

e-mail contact of main author: gerardo.giruzzi@cea.fr

**Abstract.** The modeling of the steady-state ITER scenarios is reviewed, as a subject of common work of the ITPA-SSO group. Focus is made not only on the basic physics issues, resulting from theory and experiments, but also on the difficulties and the needs of integrated modeling. Specific issues connected with high bootstrap fraction in the long pulse operation are addressed. Bootstrap current can be enhanced either by large pedestal temperatures, or by Internal Transport Barriers (ITB). Recent simulations for both high-pedestal scenarios and ITB scenarios are compared. Results of code benchmarking for typical parameters of ITER scenarios are also analyzed, and prospects for improvement of the integrated modeling capability will be discussed.

### 1. Introduction

One of the primary goals of the ITER design is to demonstrate a reactor scale long pulse operation prospective for the future tokamak reactor. Steady-state plasmas also allow to fulfil one of the basic missions of ITER, i.e., the test of tritium breeding module concepts with respect to 14 MeV neutron fluxes: these tests require a high neutron fluence ( $\geq 0.3 \text{ MWam}^{-2}$ ), which can only be attained if the tokamak can be operated in very long discharges ( $\sim 3000 \text{ s}$ ), with fusion gain  $Q \geq 5$  (the fusion gain is defined as the ratio between the power produced by the fusion reactions and the additional heating power) [1]. These requirements are challenging, because the operational space in ITER is restricted by several physical and engineering limits such as Greenwald density, beta limit, power loss to divertor, maximal edge fuelling, density limit for the Neutral Beam Injection (NBI) shinethrough loss, the maximal input power, etc. The extensive analysis of the operational space for the reference ITER inductive scenario at  $I_p = 15 \text{ MA}$ , was based on the extrapolation of a wide database of tokamak experiments. In contrast, the operational space for the steady-state has not been defined yet. The present database of tokamak discharges [2] that could be extrapolated to steady-state ITER regimes is still extremely sparse, but indicates that the existence of a high performance long pulse operation regime and its MHD stability is sensitive to the details of the current density and pressure profiles. The complex nature of these plasma scenarios

requires a substantial self-consistent integrated modeling effort in the next years to define the steady-state operational space for a variety of core and pedestal transport models.

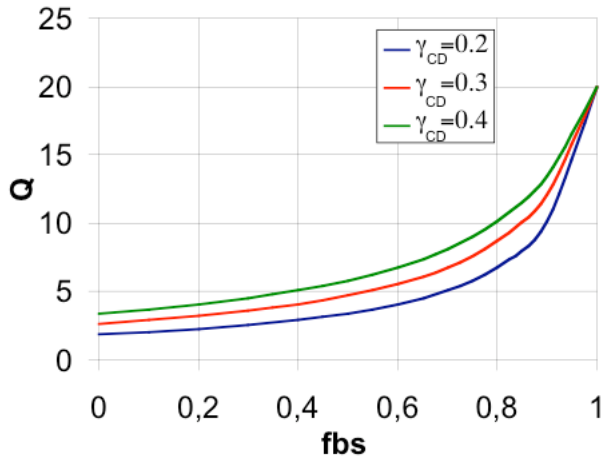


**Fig. 1:** fusion gain vs bootstrap current fraction for parameters typical of an ITER steady-state scenario. CD efficiencies are in  $A W^{-1} 10^{20} m^{-2}$

ITER steady-state scenario parameters [3] and various values of the non-inductive current drive efficiency  $\gamma_{CD}$ . In H-modes, the energy content of the plasma is naturally linked to that of the pedestal. Therefore, bootstrap current can be enhanced in two ways (not mutually exclusive): scenarios characterized by either large pedestal temperatures, or by Internal Transport Barriers (ITB).

Both classes of scenarios are confronted with common or peculiar physics problems: specific MHD phenomena, limitations related to the nature and characteristics of the power sources, control problems related to the system non-linearities. These problems are challenging not only in experiments, but also in computations, and will require a substantial integrated modeling effort in the next years. As a result, there is still no clear definition of the ITER steady-state scenario, and integrated modeling in this area is still in its infancy [4].

In this paper, the modeling of steady-state ITER scenarios is reviewed, a subject of common work in the framework of the ITPA-SSO group. Focus will be not only on the basic physics issues, resulting from theory and experiments, but also on the results and the needs of integrated modeling. Recent simulations for both high-pedestal scenarios and ITB scenarios will be presented and compared. Results of code benchmarking for typical parameters of ITER scenarios will be also analyzed, and prospects for improvement of the integrated modeling capability will be discussed.

## 2. High pedestal steady-state scenario

High pedestal scenario simulations have been developed by means of the transport code ONETWO [5] benchmarked by comparison with relevant DIII-D discharges [6], and

In fact, steady-state scenarios in ITER combine a high number of difficulties. Very long pulses can only be realized if the loop voltage is practically zero. This can always be attained for sufficiently high current drive (CD) power, but the fusion gain  $Q \geq 5$  condition limits the total auxiliary power that can be used. The simultaneous constraints on fusion performance and loop voltage can only be satisfied for high bootstrap current fractions (significantly higher than 50 %), which, in turn, require high performance plasmas, with strongly enhanced energy confinement with respect to the reference scenario. This is illustrated in Fig. 1, where the fusion gain  $Q$  is plotted vs the bootstrap fraction  $f_{bs} = I_{bs}/I_p$ , for typical

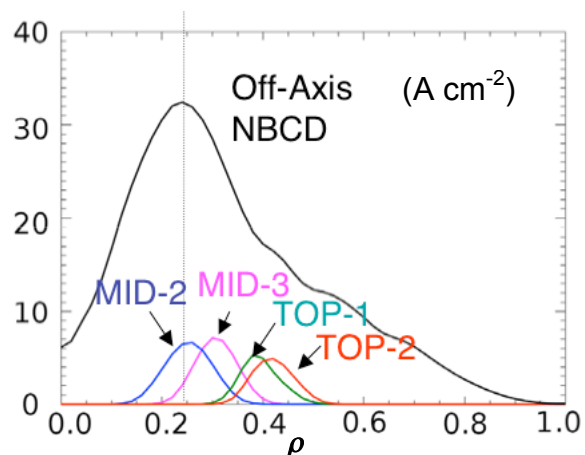


**Fig. 2:** NBCD and ECCD current sources for the high pedestal scenario

employing the theory-based transport model GLF23 [7]. ITER day-1 heating and CD capabilities are used in the simulations, i.e., 33 MW of (negative-ion based) NB power, 20 MW of ion cyclotron (IC) power, which can also provide driven current if used in the Fast Wave Current Drive (FWCD) mode, and 20 MW of electron cyclotron (EC) power. The physics of the three heating and current drive systems is modeled by means of the ray-tracing codes CURRAY [8] for FWCD and TORAY-GA [9] for EC, and the orbit-following Monte Carlo Code NUBEAM [10] for NB. In this model, the heat transport is stiff, therefore, the core temperatures are governed by the pedestal. The pressure gradient being large in the pedestal region, the bootstrap current in the pedestal provides a substantial amount of noninductive current ( $\sim 35\%$ ). The pedestal parameters are therefore crucial and have a strong impact on both requirements for the fusion gain ( $Q \geq 5$ ) and non-inductive current fraction ( $f_{\text{NI}} \approx 100\%$ ). In these simulations, the pedestal is assumed to be located at a normalized radius  $\rho = 0.9$  and  $T_{\text{ped}} = 7.8$  keV,  $n_{\text{ped}} = 0.8 \times 10^{20} \text{ m}^{-3}$ . Typical parameters are assumed for an ITER steady-state scenario:  $I_p = 9$  MA,  $B_T = 5.3$  T,  $R = 6.2$  m,  $a = 1.86$  m,  $\kappa = 1.92$ ,  $\delta = 0.43$ ,  $n_e(0) = n_{\text{ped}}$ ,  $f_{\text{Be}} = 2\%$ ,  $f_{\text{Ar}} = 0.12\%$ ,  $f_{\text{D}}/(f_{\text{D}}+f_{\text{T}}) = 0.5$ ,  $\tau_p^*/\tau_E = 5$ ,  $n_{\text{edge}} = 0.35n_e(0)$ ,  $T_{\text{edge}} = 200$  eV. Linear drops of both density and temperature in the pedestal region are assumed. The configuration of the heating systems is optimized in order to obtain the highest amount of non-inductive current fraction, while keeping the minimum safety factor above 1.5. Negative-ion based NBI is used at an energy of 1 MeV with the maximum allowable downward steering compatible with the present design of the ITER NBI system [11]. The EC power (O-mode at the frequency of 170 GHz is launched by both the equatorial and the top launcher, in order to distribute the driven

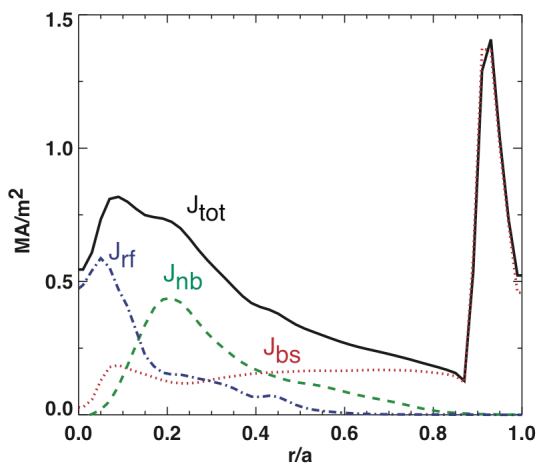


**Fig. 3:** current profiles for the high pedestal scenario

current in the region  $0.2 < \rho < 0.5$  (see Fig. 2). For IC waves, the frequency of 56 MHz is chosen in order to maximize the FWCD efficiency while minimizing the damping on alpha particles and on berillium. FWCD can provide current in the central region, which must be carefully controlled in order to keep  $q_0 - q_{\text{min}} < 0.5$ . To this end, phasing of the currents in the antenna straps is found to be an excellent control knob. An electron absorption of 65-70 % is obtained, with a maximum driven current  $I_{\text{FWCD}} = 0.53$  MA. A half of this CD capability is used in the scenario.

A stationary ( $f_{\text{NI}} = 100\%$ ) simulation is obtained [12], with a bootstrap current fraction  $f_{\text{bs}} = I_{\text{bs}}/I_p$  in excess of 70 %, for a fusion gain  $Q = 5.3$  and a normalized beta  $\beta_N = 3.1$ . The resulting current density and temperature profiles are shown in Figs. 3 and 4, respectively. The main issues concerning this scenario are related to the extrapolability of the pedestal parameters from the present database and/or from first principle pedestal simulations, to the impact of ELMs for so large pedestal

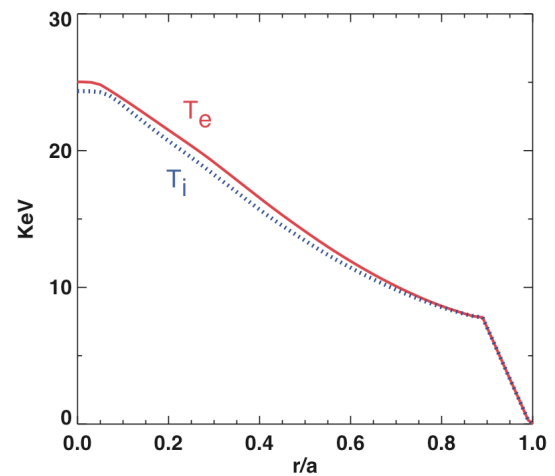


**Fig. 4:** temperature profiles for the high pedestal scenario

temperatures and to Resistive Wall Modes (owing to the large  $\beta_N$  and the broad current profile). The sensitivity of the results to variations of the pedestal temperatures have been

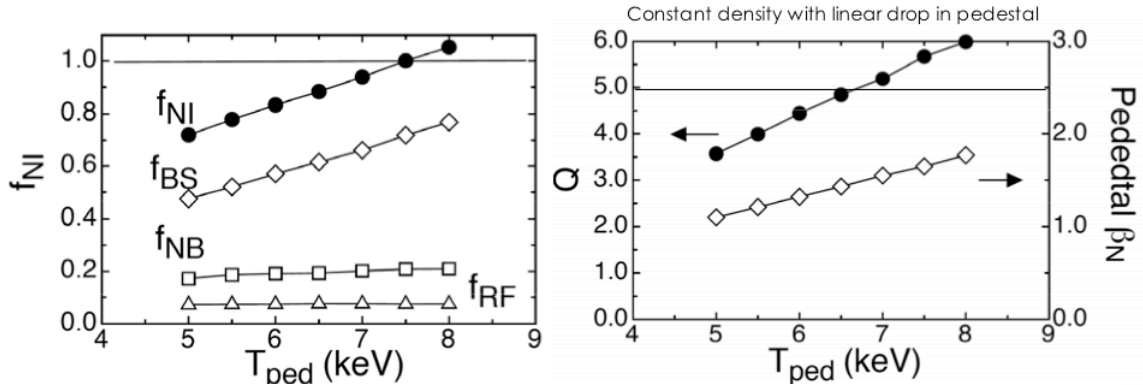


**Fig. 5:** sensitivity of various quantities to the pedestal temperature, for the high pedestal scenario

therefore explored. As shown in Fig. 5, it is found that non-inductive current fraction, bootstrap fraction and fusion gain are all linear functions of  $T_{ped}$ . It is also found that the value of normalized beta  $\beta_{Nped}$  at the pedestal required for  $f_{NI} \approx 100\%$  and  $Q \geq 5$  is significantly higher than predictions based on the EPED1 model [13]. Multi-dimensional scan of  $n_e$ ,  $T_{ped}$ ,  $I_p$  and density peaking indicates that lower  $\beta_{Nped}$  solution may be found assuming moderate density peaking and/or lower plasma current, e.g., 8 MA.

The physics of the pedestal is not the only challenge of these simulations. From the numerical point of view, the main difficulty is related to the GLF23 transport model, which provides a stiff heat diffusivity  $\chi$  (i.e., strongly dependent on the temperature gradients) and with strong radial variations. To cope with such variations, standard transport solvers usually need very small time steps, which is not convenient for simulations of 3000 s discharges. Smoothing of the heat diffusivity is only a partial solution, therefore specific solvers for stiff transport models have been developed and applied to these simulations, which allows a much faster convergence (typically 1-2 orders of magnitude) to the steady state.

### 3. Radiofrequency steady-state scenario with ITB

The second type of scenario considered combines a modest pedestal temperature with an ITB. In ITER, ITBs would be associated with negative magnetic shear rather than to rotation shear (as is the case in many present-day experiments), owing to the lack of a powerful torque source. This implies that the control of the current density profile is essential to sustain ITBs for a long time, but this is complicated when the bootstrap fraction is the dominant contribution (current alignment problem [4]). Here, results of simulations performed by the integrated modeling code CRONOS [14] are presented. A conceptual solution of the current alignment problem is proposed [15], based on the use of ECCD to lock the bootstrap current profile, a phenomenon observed in DIII-D experiments [16]. In order to model the

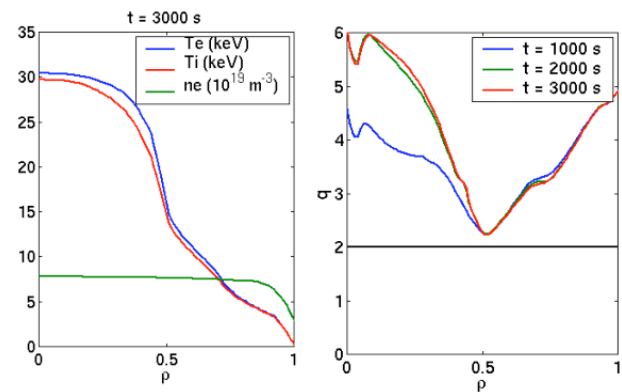


**Fig. 6:** temperatures, density and safety factor profiles for the ITB scenario

current alignment problem is proposed [15], based on the use of ECCD to lock the bootstrap current profile, a phenomenon observed in DIII-D experiments [16]. In order to model the

reduction of turbulent transport in reversed shear scenarios, a heat diffusivity model of the type used in Ref. [3] is adopted, i.e.,  $\chi_i = \chi_e = \chi_{i,neo} + 0.4(1+3\rho^2)F(s)$ , where  $F$  is a shear function (vanishing for  $s < 0$ ). This model is based on the experimental results obtained in JT-60U [17] with ITB discharges. It must be considered as a kind of minimal model which is used here to ensure that the phenomena we analyze do not depend on specific ingredients of models, but only on their common feature: the confinement improvement associated with  $s < 0$ . The pedestal temperature is fixed at  $\rho \approx 0.93$  to  $T_{ped} \approx 3$  keV, which is a conservative value, with respect to the bootstrap current generated in the edge region. The electron density profile is prescribed with a ramp in the early phase of the regime, then fixed, and the global parameters for the ITER steady-state reference scenario 4 have been considered [3], except the total current, which has been downscaled to 8 MA. The heating sources are computed in CRONOS by external modules coupled with the main transport equations. ECCD is calculated by means of REMA [18] (ray-tracing and relativistic damping of electron cyclotron waves), with a linear estimate of the ECCD efficiency [19]; LHCD is computed by LUKE/C3PO [20], i.e., a 3D Fokker-Planck code coupled to toroidal ray-tracing; ICRH is computed by means of PION [21]. The fusion power is evaluated here by the orbit following Monte-Carlo code SPOT [22].

To avoid shrinking or erosion of the ITB, a method is needed to control the dominant current component, i.e., the bootstrap current, which is in turn essentially related to the dominant heating source, i.e., the alpha heating. For such a purpose, a pure radiofrequency (RF) scenario without NBI has been considered, which is obtained using  $P_{IC} \approx 20$  MW (53 MHz, 2<sup>nd</sup> Tritium harmonic),  $P_{EC} \approx 20$  MW (170 GHz, O-mode),  $P_{LH} \approx 13$  MW (5 GHz,  $n_{||} = 2$ ). The 20 MW of EC power are deposited at  $\rho \approx 0.45$  by using 13 MW from the Upper Steering Mirrors of the Top Launcher with injection angles  $\phi_{tor} = 20^\circ$  and  $\phi_{pol} = 67^\circ$  and 8 MW from the Upper Row of the Equatorial Launcher at  $\phi_{tor} = 38^\circ$  and  $\phi_{pol} = 0^\circ$ . Using this configuration, a combination of highly peaked current density profile is obtained from the upper launcher (which is convenient for the formation of the ITB due to the magnetic shear) and broader profile from the equatorial launcher (which is convenient to have a broader ITB). The plasma density, the electron and ion temperature profiles as well as the current density profiles obtained at  $t = 3000$ s and the evolution of the  $q$  profile from  $t = 2000$ s are shown in Figs. 6 and 7. The current density profile obtained shows a maximum at  $\rho = 0.45$ , which is at the same time at the maximum of the bootstrap current and of the ECCD. Therefore, the ECCD locks the ITB at mid-radius and avoids its erosion and shrinking;

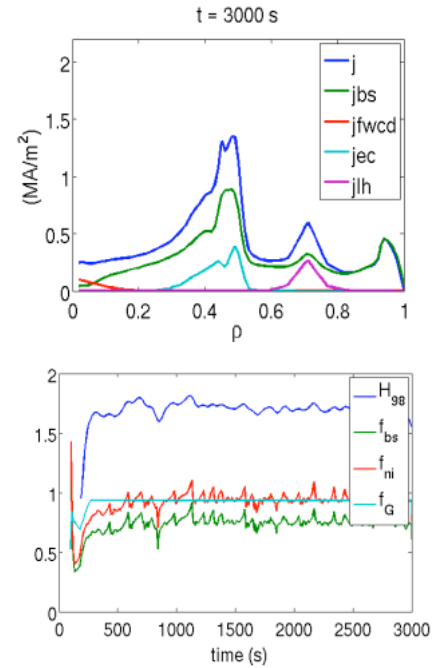


**Fig. 7:** current profiles for the ITB scenario (top); time evolution of  $H$  factor, bootstrap, non-inductive and Greenwald fractions (bottom)

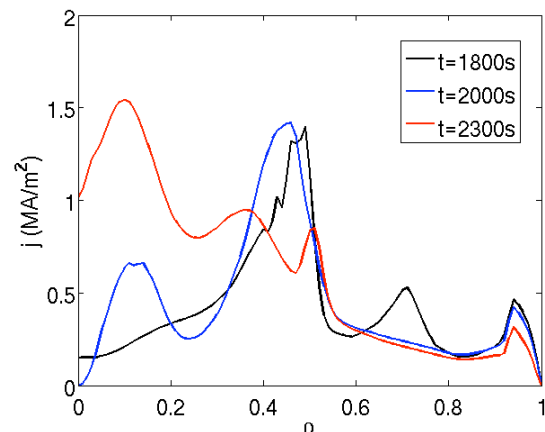


**Fig. 8:** evolution of the current density profile when LHCD is replaced by NBCD.

however, there is a clear power threshold for this feature [15]. The LH power deposition is located at  $\rho=0.7$ , and the current drive obtained ( $\approx 0.6$  MA) contributes to the total non-inductive current fraction ( $f_{NI} \approx 97\%$ ). A small amount of central current drive (e.g., by fast waves,  $I_{FWCD}=20$  kA) is added in order to control  $q_0$ . With this current drive scheme, the  $q$  profile obtained is stable for 1000s, as shown in Fig. 6, with  $q_0 \approx 6$  and  $q_{min}>2$ . With these results a fusion gain  $Q=6.5$  is obtained. The time evolution of the confinement enhancement factor with respect to the standard ITER scaling law,  $H_{98}$ , the bootstrap current fraction, the Greenwald fraction, and the total non-inductive current fraction are also shown in Fig. 7. The bootstrap current fraction ( $f_{bs}=70\%$ ) is stable during all the simulation and represents the main contribution to the total non-inductive current. The plasma is above the no-wall stability limit ( $\beta_N > 4li$ ), owing to the flatness of the current density profile, however, this feature is intrinsic to scenarios with ITB based on negative magnetic shear.

The role played by the non-inductive currents inside and outside the ITB is quite different. In fact, the LH current drive and the bootstrap current at the edge contribute to the total non-inductive current without affecting the ITB, in contrast with current sources inside the ITB. This is shown in Fig. 8, where 12MW of NBCD have been added, 12 MW of ICRH have been removed and the LHCD has been also removed to keep constant the global heating and current driven in the plasma at 1800 s. The current diffusion due to the high amount of current added inside the ITB ( $=0.7$  MA) makes the  $q$  profile drop in that region, which finally leads to the erosion of the ITB, as also obtained in other studies [4]. After the ITB is lost, the total current keeps growing in the center, and finally  $q_0 < 1$ .

In summary, this scenario provides a solution to the well known problem of current alignment, which caused the shrinking and erosion of the ITB in previous studies performed with NBCD. The present design of the EC power system in ITER can provide such a negative magnetic shear at  $\rho=0.45$  through ECCD. Nevertheless, the definition of a viable steady-state scenario for ITER still has to overcome several problematic issues. Impurity confinement and particle fuelling inside the ITB, specific MHD related to the inverted  $q$  profile (resistive interchange modes, double tearing, infernal modes), Alfvén instabilities driven by the alpha particles are the most difficult challenges, requiring extensive theoretical, computational and experimental efforts.

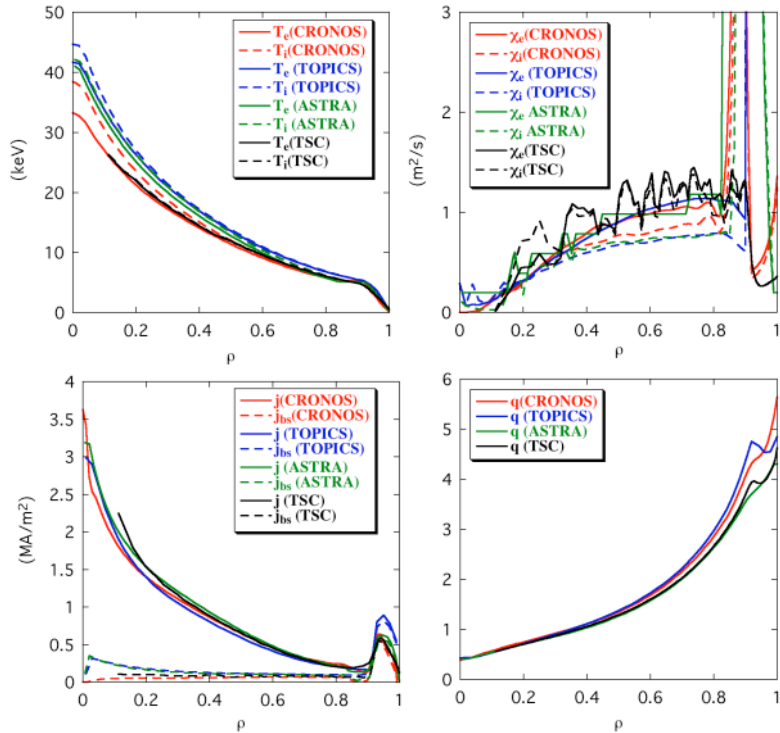


**Fig. 9:** Test case #1: comparison of temperatures, heat diffusivities, currents and safety factors computed by different codes

#### 4. Progress in integrated modeling code benchmark

Only a few integrated modeling codes are available worldwide for the challenging predictive modeling effort that is required for ITER. In the framework of the ITPA-SSO group, a benchmark activity of these codes has started. The first step of this activity consisted in running 5 of these codes for the same transport model (GLF23) and a common set of parameters (a hybrid-like ITER scenario) [23]. Although the basic characteristics of the scenario were reproduced by all the codes, substantial quantitative differences deserved further investigation. In order to discriminate the differences originating from the transport solvers from those associated with the heating sources, two additional test cases have been defined, still on the basis of the previously used parameters [23]: 1) a test case with analytically prescribed heating and CD sources (to check the temperature and current profile evolutions and the transport coefficients); 2) a test case with analytically prescribed temperatures (to check the computations of the heating sources). Four codes have participated in this benchmark: ASTRA [24], CRONOS [14], TOPICS [25] and TSC/TRANSP [26].

The main results of test case #1 are shown in Fig. 9. It appears that, although the four codes use the same transport model (GLF23), differences in its implementation and smoothing procedure cause quantitative differences of the heat diffusivities, which are eventually amplified in the time evolution (since the model depends on the temperature gradients). This causes in turn different final temperature profiles (up to 10 keV in the center). The total and bootstrap current density profiles show a satisfactory agreement. Differences of the  $q$  values in the pedestal and edge region are mainly due to differences in the geometry, which should be further investigated. The profiles of the three heating sources for the test case #2, i.e., alpha heating, NBI and ICRH, are shown in Fig. 10. Substantial differences in the alpha heating profiles are mainly due to the different Helium transport models used by the codes. The NBI deposition profiles are discussed in detail elsewhere [11]; an analogous effort on the ICRH models implemented will be definitely required in the future to solve the rather large discrepancies between codes.

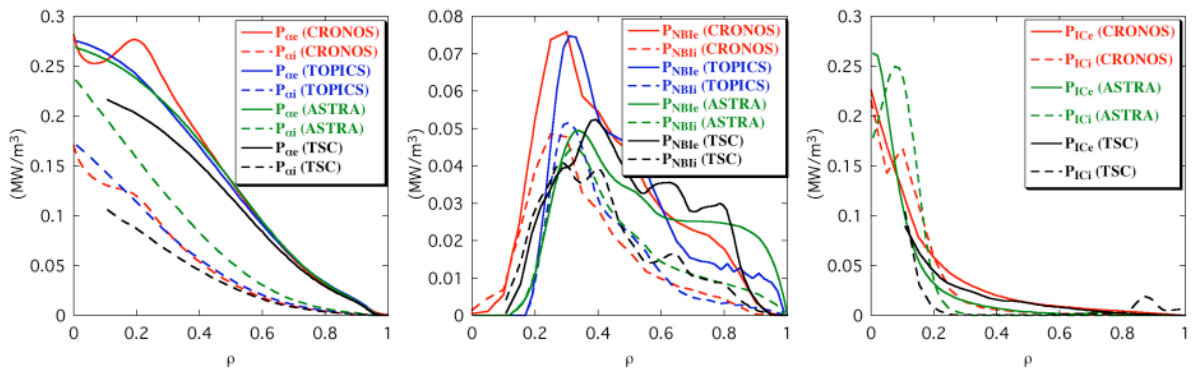


**Fig. 10:** Test case #2: comparison of heating sources computed by different codes

#### 5. Conclusions and prospects

Integrated modeling combining 1-D transport codes, 2-D self-consistent equilibria and full computation of heating and CD sources finds its best application in the development of steady-state scenarios, which are critically dependent on details of both plasma quantities and sources profiles. It is clear that this is the way to be followed in order to progress in the definition of a viable steady-state scenario for ITER. However, predictive simulation of 3000 s discharges with theory-based transport and sources models is presently a challenging

computational task, which typically requires several days or weeks on a small-sized computer cluster. These simulations do not yet include essential physics ingredients, such as, e.g., theory-based pedestal models and self-consistent evaluation of the relevant MHD limits, which constitute the main constraint on this type of scenarios. Despite these substantial limitations, progress has been made in the definition of steady-state scenarios for ITER. The two extreme cases presented here, i.e., high-pedestal and purely RF, ITB scenario, still have substantial drawbacks, but show possible solutions to the current alignment problem.

In view of the impressive amount of work that can be foreseen, and that is necessary, in the next years, it is now clear that technical improvement of the numerical performances and of the physics content of the codes will be a strategic issue. A thorough benchmark of the codes is also a necessary step. Although the various ITER partners have ambitious projects in this area, a significant enhanced cooperation effort among partners appears necessary and urgent. The ITPA-SSO activity has been a first modest step in this direction, which is far from being sufficient. Real progress will require a more intensive and coordinated effort.

**Acknowledgements.** This report was prepared as an account of work by or for the ITER Organization. The Members of the Organization are the People's Republic of China, the European Atomic Energy Community, the Republic of India, Japan, the Republic of Korea, the Russian Federation, and the United States of America. The views and opinions expressed herein do not necessarily reflect those of the Members or any agency thereof. Dissemination of the information in this paper is governed by the applicable terms of the ITER Joint Implementation Agreement.

Part of this work, supported by the European Communities under the contract of Association between EURATOM and CEA, was carried out within the framework of the European Fusion Development Agreement. The views and opinions expressed herein do not necessarily reflect those of the European Commission.

Part of this work was supported by DoE Contract No. DE-AC02-76-CH0-3073.

- [1] M. Shimada et al., Nucl. Fusion **47**, S18 (2007).
- [2] P. Gohil et al., Nucl. Fusion **43** (2003) 708.
- [3] Polevoi A.R. et al 2002 Proc. 19th Int. Conf. on Fusion Energy (Lyon, 2002) (Vienna: IAEA) IAEA-CN-94/CT/P-08 CD-ROM
- [4] W. Houlberg et al, Nucl. Fusion **45** (2005) 1309
- [5] H.E. St. John et al., Proc. 15th Int. Conf. on Fusion Energy (Seville, 1994), P5.037.
- [6] M. Murakami et al., Nucl. Fusion **45** (2005) 1419.
- [7] J.E. Kinsey et al., Phys. Plasmas **12** (2005) 052503.
- [8] T.K. Mau et al., Proc. EPS Top. Conf. on RF Heating and CD of Fusion Devices (Brussels, 1982), vol. 16E, p. 181.
- [9] K. Matsuda, IEEE Trans. Plasma Sci. **17** (1989) 6.
- [10] A. Pankin et al., Comput. Phys. Commun. **159** (2004) 157.
- [11] T. Oikawa et al., this conference, IT/P6-5.
- [12] J. M. Park, IEA/W68 Workshop on Development of High  $\beta_N$  Scenario for ITER, San Diego, June 24-25, 2008.
- [13] P.B. Snyder et al., this conference, IT/P6-14.
- [14] V. Basiuk et al., Nucl. Fusion **43** (2003) 822.
- [15] J. Garcia et al., Phys. Rev. Lett. **100** (2008) 255004.
- [16] M. Murakami et al., Phys. Rev. Lett. **90** (2003) 255001.
- [17] T. Fujita et al., Phys. Rev. Lett. **78** (1997) 2377.
- [18] V. Krivenski et al., Nucl. Fusion **25** (1985) 127.
- [19] Y.R. Lin-Liu et al., Phys. Plasmas **10** (2003) 4064.
- [20] Y. Peysson and J. Decker in Proc. of the 34th EPS Conf. on Contr. Fusion and Plasma Phys., Warsaw 2007 (EPS, Paris, 2007).
- [21] L.G. Eriksson et al, Nucl. Fusion **33** (1993) 1037.
- [22] M. Schneider et al., Plasma Phys. Control. Fusion **47** (2005) 2087.
- [23] C.E. Kessel et al., Nucl. Fusion **47** (2007) 1274.
- [24] G. Pereverzev et al., IPP-Report IPP 5/98 (2002).
- [25] N. Hayashi et al., Nucl. Fusion **45** (2005) 933.
- [26] C.E. Kessel et al., Phys. Plasmas **13** (2006) 056108.